

## Research article

---

### Investigating Transit Timing Variations of a Hot Jupiter HAT-P-43 b

Muhammadalawee Sareh<sup>1</sup>, Supachai Awiphan<sup>2</sup>, Napaporn A-thano<sup>2</sup>,  
Siramas Komonjinda<sup>1</sup> and Eamonn Kerins<sup>3</sup>

<sup>1</sup>Department of Physics and Materials Science, Faculty of Science, Chiang Mai University,  
Chiang Mai, 50200, Thailand

<sup>2</sup>National Astronomical Research Institute of Thailand (Public Organization), Chiangmai,  
50180, Thailand

<sup>3</sup>Jodrell Bank Centre for Astrophysics, Department of Physics and Astronomy,  
The University of Manchester, Manchester M13 9PL, UK

Received: 5 January 2025, Revised: 6 March 2025, Accepted: 14 April 2025, Published: 30 May 2025

#### Abstract

HAT-P-43 b is a hot Jupiter exoplanet that orbits a late-F-type host star with a period of 3.332687 days. In this work, we present a detailed analysis of HAT-P-43 b using 47 light curves from the Transiting Exoplanet Survey Satellite (TESS), 9 light curves from the Kepler space telescope, four light curves from the Thai Robotic Telescopes (TRTs), and 4 previously published light curves from Boisse et al. (2013). The light curves were analyzed to derive HAT-P-43 b's physical parameters and mid-transit times for each transit using the TransitFit package. Using the newly derived mid-transit times, the transit timing variations (TTV) of HAT-P-43 b were analyzed. To detect the periodicity of the TTV signal, a Generalized Lomb-Scargle (GLS) periodogram was created using the mid-transit times. The analysis revealed a peak at 0.184146 cycles per period, corresponding to a period of 5.43046 periods per cycle, with a false alarm probability (FAP) of 0.54%. Although a low FAP was obtained, the sinusoidal fitting of the HAT-P-43 b TTV did not match well, making it difficult to draw a definitive conclusion about the presence of a third body. Therefore, future observational data will be valuable in confirming whether a third body exists in this system.

**Keywords:** exoplanets; transit; hot Jupiter; transit timing variations

#### 1. Introduction

In recent years, the study of exoplanetary systems has grown rapidly, with more than 5,800 exoplanetary systems discovered to date. These discoveries have contributed to our understanding of the formation and evolution of exoplanetary systems and offer valuable insights into the potential for life beyond Earth. To date, most exoplanets have been discovered using the transit technique, which provides critical information about planetary

---

\*Corresponding author: E-mail: siramas.k@cmu.ac.th  
<https://doi.org/10.55003/cast.2025.265878>

Copyright © 2024 by King Mongkut's Institute of Technology Ladkrabang, Thailand. This is an open access article under the CC BY-NC-ND license (<http://creativecommons.org/licenses/by-nc-nd/4.0/>).

orbits and radii. However, this method has limitations, as it requires the planet to transit in front of its host star during the observation period. Consequently, detecting planets with low orbital inclinations or long orbital periods is challenging (Udry & Nuno, 2007).

To overcome these limitations, transit timing variations (TTVs) are used to detect additional planets within a system. By measuring variations in the transit times of known planets, TTVs can reveal the presence of other planets exerting gravitational influences. Additionally, TTVs can be used to estimate planetary masses (Agol et al., 2005) and to characterize their key orbital properties, such as eccentricity and long-term dynamical changes (Nesvorný & Morbidelli, 2008).

In our research, we focus on HAT-P-43 b, located at RA 08h 35m 42.17s and DEC +10° 12' 23.92", approximately 528.825 parsecs away. HAT-P-43 has an effective temperature of 5645 K, a metallicity of  $[Fe/H] = 0.23 \pm 0.08$ , and a surface gravity of  $\log(g) = 4.37$  cgs. The orbital period of this planet is 3.332687 days, and it orbits its host star at a semi-major axis of 8.64 stellar radii. It has a mass of approximately 0.662 Jupiter masses and a radius of about 1.281 Jupiter radii (Boisse et al., 2013). Since the discovery paper by Boisse et al. (2013), this planet has not been extensively studied. Due to its short orbital period and low density, it can be assumed that the planet has undergone migration and may have additional planets in the system that could influence its orbit (Li et al., 2022).

In this study, we analyze TTV signals and orbital period variations of HAT-P-43 b to investigate the possibility of additional objects within this exoplanetary system. Our analysis combines data from the Transiting Exoplanet Survey Satellite (TESS), the Kepler mission archives, and observations from Thai Robotic Telescopes (TRTs), along with findings reported by Boisse et al. (2013).

## 2. Materials and Methods

### 2.1 Observational data

In this work, we present photometric observations of the exoplanet HAT-P-43 b, which were analyzed using data from TESS (*TESS* band), Kepler (*Kepler* band), TRT-SBO (*R*-band), and ROP-CC telescope (*V*-band), as shown in Table 1. Additionally, we combined these data with those from Boisse et al. (2013) to refine the planetary parameters of HAT-P-43 b using multi-band observations.

**Table 1.** Log of Observations of HAT-P-43 b Transits from ROPCC and TRT-SBO telescopes. Epoch=0 is the transit on 2012 March 10<sup>th</sup>.

Observation Date	Telescope	Epoch	Filter
16 <sup>th</sup> Jan 2019	ROP-CC	751	V
5 <sup>th</sup> Feb 2019	ROP-CC	757	V
15 <sup>th</sup> Feb 2019	ROP-CC	760	V
14 <sup>th</sup> Feb 2021	TRT-SBO	979	R

#### 2.1.1 TESS telescope

The Transiting Exoplanet Survey Satellite (TESS), a space observatory dedicated to exoplanetary surveys, is equipped with four wide-field lenses that cover a 24×90-degree field and a waveband of approximately 600 to 1000 nm (Ricker et al., 2014). In this work, we analyzed 47 light curves of HAT-P-43 b from seven TESS sectors: Sector 7 in 2019,

and Sectors 34, 44, 45, 46, 61, and 72 in 2021. These sectors were chosen because they include all of the HAT-P-43 b observations that are currently available. In order to improve transit recognition and optimize temporal resolution, we also prioritized data with the shortest exposure time.

### **2.1.2 Kepler telescope**

The Kepler space telescope, designed for exoplanetary surveys, has a 1.4-m primary mirror and primarily observes in the visible to near-infrared wavelengths (400 to 850 nm) (Koch et al., 2010). Nine light curves of HAT-P-43 b were obtained during the K2 mission of Kepler in 2018.

### **2.1.3 ROP-CC 0.7-m telescope**

The ROP-CC is a 0.7m telescope located at the Regional Observatory for the Public (Chachoengsao). Two full transits and one partial light curve of HAT-P-43 b were obtained in the V-band filter in 2019.

### **2.1.4 TRT-SBO 0.7-m**

The TRT-SBO telescope is a 0.7m telescope located at the Spring Brook Observatory in Australia, which is part of the Thai Robotic Telescope Network. One full transit of HAT-P-43 b was observed using the TRT-SBO Telescope in 2021.

### **2.1.5 Previously published data from Boisse et al. (2013)**

Boisse et al. (2013) published four light curves of HAT-P-43 b using three instruments: HAT-5, HAT-6, and HAT-7, which are located at the Fred Lawrence Whipple Observatory (FLWO) in Arizona, USA, and HAT-8, located at the Mauna Kea Observatory in Hawaii, USA. These observations were made using the  $r'$  and  $i'$  band filters with KeplerCam on the FLWO 1.2m telescope in 2010 and 2011.

## **2.2 Light curve fitting**

We used the TransitFit package (Hayes et al., 2023), a software designed to fit multiband and multi-epoch data in exoplanet transit observations to obtain the best-fit light curves and planetary parameters of HAT-P-43 b. TransitFit utilizes the transit model from Batman (Kreidberg, 2015) and employs the dynamic nested sampling routines from Dynesty (Speagle, 2020) to determine the parameters of HAT-P-43 b.

We used TransitFit to analyze 64 light curves of HAT-P-43 b, detrending each transit independently using a second-order polynomial detrending technique. The priors used for modeling the planet's parameters are shown in Table 2. The limb-darkening coefficients were determined by TransitFit in the "Coupled" mode for each filter. This mode allows for the simultaneous fitting of limb-darkening coefficients across multiple wavelengths, using the quadratic limb-darkening model derived from the Limb Darkening Toolkit (LDTK; Parviainen & Aigrain, 2015). Additionally, priors on the host star properties were included, adopting an effective temperature ( $T_{\text{eff}}$ ) of 5645 K and  $\log g = 4.37 \pm 0.02$  cgs (Boisse et al., 2013).

**Table 2.** Initial planetary parameters of HAT-P-43 b used for transit light curves modelling

Parameter	Distribution	Value	Filter
$P(\text{days})$	Fixed	3.3326820	
$t_0(\text{BJD}_{\text{TDB}})$	Gaussian	$2455997.3710 \pm 0.0003$	
$a/R_*$ (star radii)	Uniform	(7,9)	
$\text{Inclination}(\text{degree})$	Uniform	(87,89)	
$R_p/R_*$	Uniform	(0.11,0.13)	TESS
$R_p/R_*$	Uniform	(0.11,0.13)	Kepler
$R_p/R_*$	Uniform	(0.11,0.13)	V
$R_p/R_*$	Uniform	(0.11,0.13)	i'
$R_p/R_*$	Uniform	(0.11,0.13)	R
$\text{Eccentricity}$	Fixed	0	

### 2.3 Transit timing variation analyses

The Transit Timing Variation (TTV) analysis of HAT-P-43 b was performed using 64 mid-transit times obtained from TransitFit. The linear ephemeris of HAT-P-43 b was determined using the following linear ephemeris model;

$$T_m^c = T_{0,l} + E \times P_l, \quad (1)$$

where  $T_{0,l}$  is the reference time,  $P_l$  is the linear ephemeris model's orbital period, and  $E$  is the epoch number.  $T_m^c(E)$  represents the determined mid-transit time for a given epoch  $E$ . We obtained an updated linear ephemeris of HAT-P-43 b as;

$$T_m^c = 2455997.37086 + E \times 3.33268, \quad (2)$$

Using a new linear ephemeris from equation 2, the O-C diagram is constructed in Figure 1 to search for gravitational interactions from a third body in the system. The periodic signal detected in the frequency analysis may indicate gravitational perturbations caused by an unseen object. If an additional planet exists near HAT-P-43 b, interactions between the two bodies could induce periodic variations in the planet's transit timing. Over multiple transits, these variations could accumulate and manifest as a detectable periodic signal (Holman & Murray, 2005; Agol & Fabrycky, 2018). Therefore, the Generalized Lomb-Scargle Periodogram (GLS) (Zechmeister & Kürster, 2009) is employed to analyze the periodicity of the timing residuals (O-C) data shown in Table 3.

However, the frequency of the maximum power peak is evaluated under the assumption of sinusoidally variable TTVs, following the process outlined in von Essen et al. (2019). We then use the frequency and amplitude values derived from the TTV analysis with the GLS to fit a sine function to the timing residuals (O-C) data, with the epoch in phase format as a function:

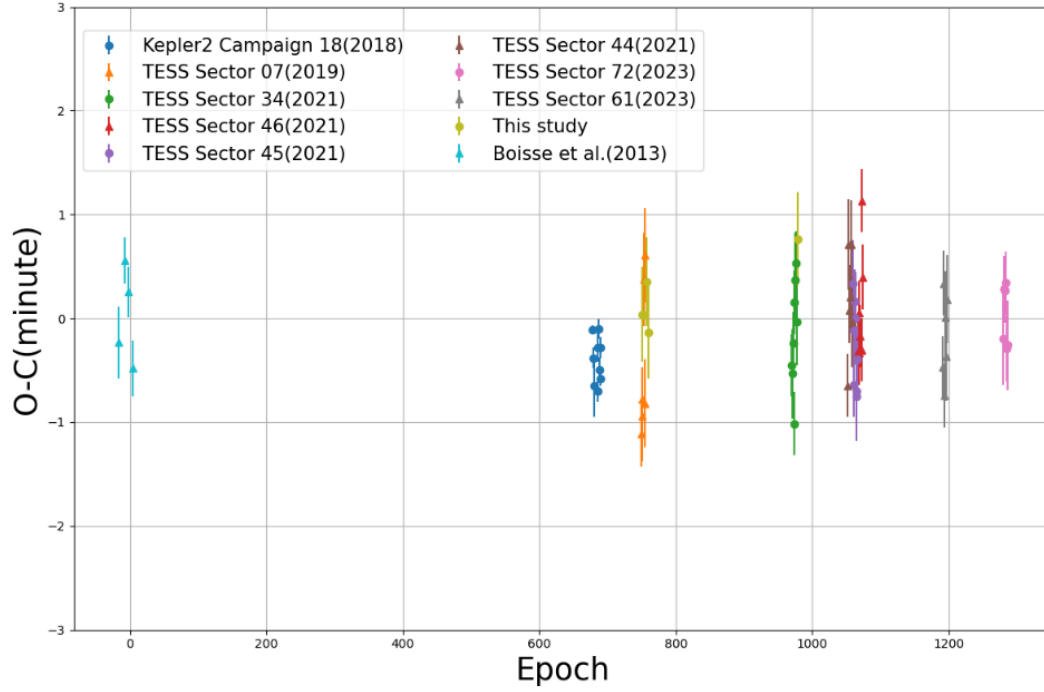


**Figure 1.** O-C diagram of HAT-P-43 b

$$TTV(E) = A_{TTV} \cdot \sin(2\pi f t - \phi), \quad (3)$$

where  $A_{TTV}$  is the amplitude (min) of the timing perturbation,  $f$  is the frequency associated with the highest peak in the power periodogram, and  $\phi$  is the phase. The O-C data were plotted with a period, forming a sine wave fitted by equation 3.

### 3. Results and Discussion

The fitted period obtained was  $P = 3.332682$  days. This fitted period is used to model the light curve and determine the mid-transit time for each epoch. The fitted planetary parameters of HAT-P-43 b, shown in Table 4, include an inclination of  $i = 89.8^\circ$  and a star-planet separation of  $8.72 R_*$ . These derived parameters are consistent with the values reported by Boisse et al. (2013). The resulting fitted light curves from the ROP-CC and TRT-SBO telescopes are shown in Figure 2, highlighting the quality of our observational data.

**Table 3.** Timing residual (O-C) from 64 light curves of HAT-P-43 b

Epoch	O-C (min)	Error (min)	Telescope	Epoch	O-C (min)	Error (min)	Telescope
-17	-0.23409	0.34848	Boisse et al., 2013	1053	0.70908	0.43438	TESS sector 44
-7	-0.23409	0.34848	Boisse et al., 2013	1054	0.07541	0.31282	TESS sector 44
-2	0.25363	0.24604	Boisse et al., 2013	1056	0.20897	0.30706	TESS sector 44
4	-0.48152	0.26940	Boisse et al., 2013	1057	0.71247	0.42243	TESS sector 44
678	-0.11246	0.04469	Kepler	1058	-0.03192	0.43923	TESS sector 44
679	-0.38225	0.09740	Kepler	1059	0.33103	0.42501	TESS sector 45
680	-0.65038	0.30121	Kepler	1060	-0.12139	0.44083	TESS sector 45
685	-0.70488	0.09514	Kepler	1061	-0.64297	0.30694	TESS sector 45
686	-0.27842	0.14257	Kepler	1062	0.16587	0.30677	TESS sector 45
687	-0.10168	0.09213	Kepler	1063	-0.00259	0.44490	TESS sector 45
688	-0.49923	0.12497	Kepler	1064	-0.69667	0.31039	TESS sector 45
689	-0.28093	0.10096	Kepler	1065	-0.74861	0.43131	TESS sector 45
690	-0.58166	0.06352	Kepler	1066	-0.39489	0.31807	TESS sector 45
749	-1.11312	0.31598	TESS sector 07	1067	-0.31193	0.30829	TESS sector 46
750	-0.78005	0.30925	TESS sector 07	1068	0.04897	0.30746	TESS sector 46
751	-0.93845	0.44154	TESS sector 07	1069	-0.32996	0.31341	TESS sector 46
751	0.03820	0.46077	ROPCC	1070	-0.17052	0.30201	TESS sector 46
753	0.37459	0.44707	TESS sector 07	1072	-0.30368	0.30383	TESS sector 46
754	0.60620	0.45413	TESS sector 07	1073	1.13171	0.30299	TESS sector 46
755	-0.81660	0.42067	TESS sector 07	1074	0.39799	0.30989	TESS sector 46
757	0.34884	0.42680	ROPCC	1191	-0.46804	0.30083	TESS sector 61
760	-0.13778	0.44408	ROPCC	1192	0.33810	0.30940	TESS sector 61
970	-0.44932	0.53217	TESS sector 34	1193	-0.74051	0.30879	TESS sector 61
971	-0.53291	0.43442	TESS sector 34	1195	0.00834	0.44531	TESS sector 61
972	-0.23698	0.29692	TESS sector 34	1196	-0.36289	0.43438	TESS sector 61
973	-1.01504	0.30259	TESS sector 34	1197	0.18425	0.42506	TESS sector 61
974	0.15376	0.31102	TESS sector 34	1280	-0.19999	0.44453	TESS sector 72
975	0.37102	0.44839	TESS sector 34	1281	0.28148	0.26487	TESS sector 72
976	0.53217	0.30500	TESS sector 34	1282	0.26487	0.30933	TESS sector 72
977	-0.02945	0.42509	TESS sector 34	1284	0.33977	0.30228	TESS sector 72
979	0.76421	0.44768	TRT-SBO	1285	-0.29153	0.31417	TESS sector 72
1052	-0.64572	0.30041	TESS sector 44	1286	-0.25953	0.43274	TESS sector 72

**Table 4.** Output planetary parameters of HAT-P-43 b from TransitFit

Parameter	Value	Error	Filter
$P(\text{days})$	3.332682		
$a/R_*$ (star radii)	8.72	0.02	
Inclination (degree)	89.8	0.2	
$R_p/R_*$	0.1160	0.0001	TESS
$R_p/R_*$	0.1125	0.0003	Kepler
$R_p/R_*$	0.1207	0.0005	V
$R_p/R_*$	0.1202	0.0002	$i'$
$R_p/R_*$	0.1100	0.0005	R
Eccentricity	0		
$u0$	0.525	0.002	TESS
$u0$	0.527	0.002	Kepler
$u0$	0.526	0.002	V
$u0$	0.526	0.002	$i'$
$u0$	0.526	0.002	R
$u1$	0.136	0.002	TESS
$u1$	0.134	0.002	Kepler
$u1$	0.134	0.002	V
$u1$	0.134	0.002	$i'$
$u1$	0.134	0.002	R

To investigate possible transit timing variations (TTVs), a Generalized Lomb-Scargle (GLS) periodogram analysis was performed on the mid-transit times. The analysis revealed a maximum power peak at a frequency of 0.184146 cycles/period, corresponding to a period of approximately 5.43046 periods/cycle, with a false alarm probability (FAP) of 0.54%. The TTV data are shown in Figure 3. This suggests a potential periodic signal within the TTV data.

Despite the presence of this periodic signal, the reduced chi-square ( $\chi^2_{\text{red}}$ ) value from the fitting was calculated to be 4.611, which indicates a relatively poor fit. This high chi-square value implies that it is not statistically significant enough to confirm the presence of a genuine TTV signal. The lack of a clear, significant TTV signal in the HAT-P-43 system is further supported by Figure 4, where no distinct pattern or periodicity can be found in the TTV residuals.

However, it is important to emphasize that this interpretation remains speculative at this stage, given the relatively low FAP and the absence of a clear periodicity pattern. Further follow-up observations of HAT-P-43 b, particularly high-precision transit monitoring and radial velocity measurements, will be essential to investigate this possibility and detect any additional planets in more detail.

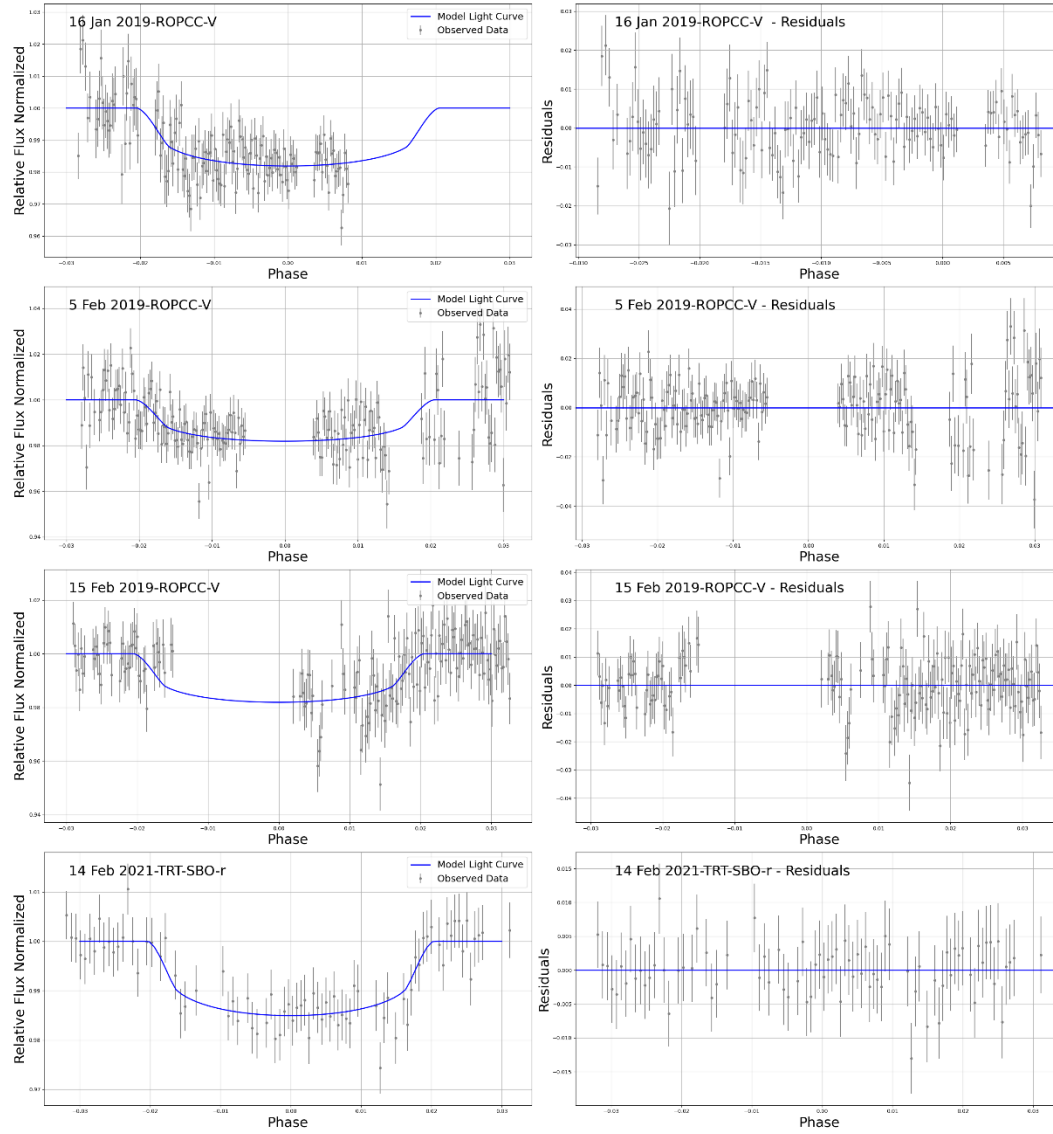


**Figure 2.** Normalized, phase-folded transit light curves of HAT-P-43 b observed using the ROPCC and TRT-SBO telescopes (represented by gray dots), along with the best-fitting model derived from TransitFit (blue solid lines) in the left panels. The right panels illustrate the corresponding residual light curves after subtracting the models. Both the light curves and the residuals include arbitrary vertical offsets for clarity.



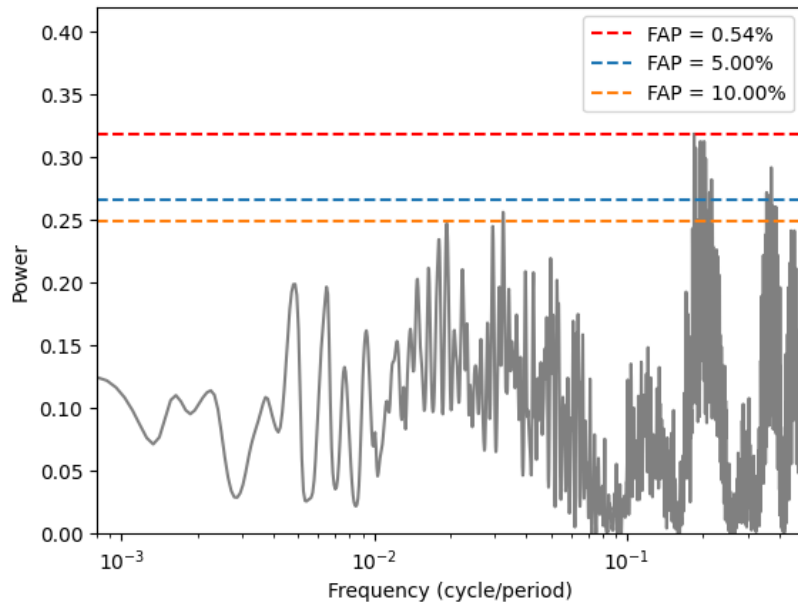


**Figure 3.** TTV signal of HAT-P-43 b from Generalized Lomb-Scargle Periodogram. The frequency of 0.184146 cycles/epoch at the highest power peak of 0.318540, with FAP = 0.54%.

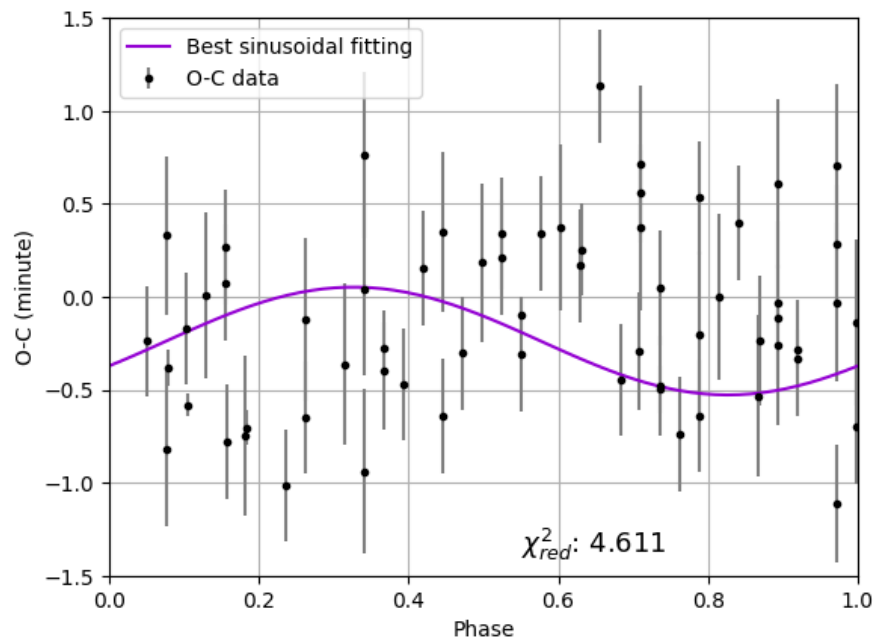


**Figure 4.** O-C diagram and the best fit of the sinusoidal variability from the frequency of the highest power peak at 0.184146 cycles/epoch, where FAP = 0.54%.

## 4. Conclusions

In this study, we investigated the transit timing variations (TTVs) of the exoplanet HAT-P-43 b using transit data from the TESS and K2 missions, along with published light curves and additional observations from a Thai telescope. By fitting these light curves with TransitFit, we derived mid-transit times and constructed O-C diagrams for further analysis. Applying the Generalized Lomb-Scargle Periodogram (GLS) to the O-C data revealed a significant peak at a frequency of 0.184146 cycles/period, with a false alarm probability (FAP) of 0.54%. However, given this relatively high FAP and the reduced chi-squared value of 4.611 from our sinusoidal fit, we consider the detection of a periodic TTV signal to be tentative at best.

The detected periodicity could suggest the presence of an additional body in the HAT-P-43 system, but no previous study has specifically analyzed TTV signals for HAT-P-43 b. Our study is the first attempt to investigate such variations, as previous works on this system primarily focused on determining basic planetary parameters, such as orbital period and radius. Notably, our derived parameters show good agreement with those reported in earlier works by Boisse et al. (2005). Although similar TTV signatures have been observed in other hot Jupiter systems (Korth et al., 2024), the current data for HAT-P-43 b are insufficient to draw a firm conclusion. It is also possible that the apparent periodicity results from a combination of stellar activity, instrumental systematics, or atmospheric effects during ground-based observations (Agol & Fabrycky, 2018).

We therefore recommend further high-precision transit timing observations and complementary radial velocity measurements. These follow-up efforts are essential to confirm the presence of long-term TTVs in HAT-P-43 b. Our study highlights the importance of such monitoring for systems with relatively limited historical transit data.

## 5. Acknowledgements

This work was supported by National Astronomical Research Institute of Thailand (NARIT) and Thailand Science Research and Innovation (TSRI) research grant. This work was also supported by the Development and Promotion of Science and Technology (DPST) Scholarship.

## 6. Authors' Contribution

S.A. and S.K.; Conceptualization. M.S, S.A, N.A., S.K, and E.K.; Methodology. M.S., S.A. and N.A.; Formal analysis. M.S.; Writing – original draft preparation. S.A., N.A., and S.K.; Writing – Review & editing. S.A. and S.K.; Supervision.

## 7. Conflicts of Interest


The authors declare that there is no conflict of interest.

### ORCID

Supachai Awiphan  <https://orcid.org/0000-0003-3251-3583>

Napaporn A-thano  <https://orcid.org/0000-0001-7234-7167>

Siramas Komonjinda  <https://orcid.org/0000-0001-7987-017X>

Eamonn Kerins  <https://orcid.org/0000-0002-1743-4468>

## References

- Agol, E., & Fabrycky, D. C. (2018). Transit-Timing and duration variations for the discovery and characterization of exoplanets. In H. Deeg, & J. Belmonte (Eds.). *Handbook of exoplanets* (pp. 797-816). Springer. [https://doi.org/10.1007/978-3-319-55333-7\\_7](https://doi.org/10.1007/978-3-319-55333-7_7)
- Agol, E., Steffen, J., Sari, R., & Clarkson, W. (2005). On detecting terrestrial planets with timing of giant planet transits. *Monthly Notices of the Royal Astronomical Society*, 359(2), 567-579. <https://doi.org/10.1111/j.1365-2966.2005.08922.x>
- Boisse, I., Hartman, J. D., Bakos, G. Á., Penev, K., Csubry, Z., Béky, B., Latham, D. W., Bieryla, A., Torres, G., Kovács, G., Buchhave, L. A., Hansen, T., Everett, M., Esquerdo, G. A., Szklenár, T., Falco, E., Shporer, A., Fulton, B. J., Noyes, R. W., Stefanik, R. P., Papp, I., . . . Sári, P. (2013). HAT-P-42b and HAT-P-43b. Two inflated transiting hot Jupiters from the HATNet survey. *Astronomy and Astrophysics*, 558, Article A86. <https://doi.org/10.1051/0004-6361/201220993>
- Hayes, J. J. C., Priyadarshi, A., Kerins, E., Awiphan, S., McDonald, I., A-Thano, N., Morgan, J. S., Humpage, A., Charles, S., Wright, M., Joshi, Y. C., Jiang, I., Inyanya, T., Padjaroen, T., Munsaket, P., Chuanraksasat, P., Komonjinda, S., Kittara, P., Dhillon, V. S., Marsh, T. R., Reichart, D. E., . . . Poshyachinda, S. (2023). TransitFit: combined multi-instrument exoplanet transit fitting for JWST, HST, and ground-based transmission spectroscopy studies. *Monthly Notices of the Royal Astronomical Society*, 527(3), 4936-4954. <https://doi.org/10.1093/mnras/stad3353>
- Holman, M. J., & Murray, N. W. (2005). The use of transit timing to detect Terrestrial-Mass extrasolar planets. *Science*, 307(5713), 1288-1291. <https://doi.org/10.1126/science.1107822>
- Li, Z., Kane, S. R., Dalba, P. A., Howard, A. W., & Isaacson, H. T. (2022). New dynamical state and habitability of the HD 45364 planetary system. *The Astronomical Journal*, 164(4), Article 163. <https://doi.org/10.3847/1538-3881/ac8d63>
- Koch, D. G., Borucki, W. J., Basri, G., Batalha, N. M., Brown, T. M., Caldwell, D., Christensen-Dalsgaard, J., Cochran, W. D., DeVore, E., Dunham, E. W., Gautier, T. N., Geary, J. C., Gilliland, R. L., Gould, A., Jenkins, J., Kondo, Y., Latham, D. W., Lissauer, J. J., Marcy, G., Monet, D., Sasselov, D., . . . Wu, H. (2010). *Kepler mission* design, realized photometric performance, and early science. *The Astrophysical Journal Letters*, 713(2), L79-L86. <https://doi.org/10.1088/2041-8205/713/2/L79>
- Korth, J., Chaturvedi, P., Parviainen, H., Carleo, I., Endl, M., Guenther, E. W., Nowak, G., Persson, C. M., MacQueen, P. J., Mustill, A. J., Cabrera, J., Cochran, W. D., Lillo-Box, J., Hobbs, D., Murgas, F., Greklek-McKeon, M., Kellermann, H., Hébrard, G., Fukui, A., Pallé, E., Jenkins, J. M., . . . Winn, J. N. (2024). TOI-1408: Discovery and photodynamical modeling of a small inner companion to a hot Jupiter revealed by transit timing variations. *The Astrophysical Journal Letters*, 971(2), Article L28. <https://doi.org/10.3847/2041-8213/ad65fd>
- Kreidberg, L. (2015). Batman: BASic Transit model cAlculationN in Python. *Publications of the Astronomical Society of the Pacific*, 127(957), 1161-1165. <https://doi.org/10.1086/683602>
- Nesvorný, D., & Morbidelli, A. (2008). Mass and orbit determination from transit timing variations of exoplanets. *The Astrophysical Journal*, 688(1), 636-646. <https://doi.org/10.1086/592230>
- Parviainen, H., & Aigrain, S. (2015). LDTK: Limb darkening toolkit. *Monthly Notices of the Royal Astronomical Society*, 453(4), 3822-3827. <https://doi.org/10.1093/mnras/stv1857>
- Ricker, G. R., Winn, J. N., Vanderspek, R., Latham, D. W., Bakos, G. Á., Bean, J. L., Bert-Thompson, Z. K., Brown, T. M., Buchhave, L., Butler, N. R., Butler, R. P., Chaplin, W.

- J., Charbonneau, D., Christensen-Dalsgaard, J., Clampin, M., Deming, D., Doty, J., De Lee, N., Dressing, C., Dunham, E. W., . . . Villaseñor, J. (2014). Transiting exoplanet survey satellite (TESS). *Proceedings of SPIE, the International Society for Optical Engineering/Proceedings of SPIE*, 9143, 914320. <https://doi.org/10.1117/12.2063489>
- Speagle, J. S. (2020). Dynesty: a dynamic nested sampling package for estimating Bayesian posteriors and evidences. *Monthly Notices of the Royal Astronomical Society*, 493(3), 3132-3158. <https://doi.org/10.1093/mnras/staa278>
- Udry, S., & Santos, N. C. (2007). Statistical properties of exoplanets. *Annual Review of Astronomy and Astrophysics*, 45, 397-439. <https://doi.org/10.1146/annurev.astro.45.051806.110529>
- von Essen, C., Wedemeyer, S., Sosa, M. S., Hjorth, M., Parkash, V., Freudenthal, J., Mallonn, M., Miculán, R. G., Zibecchi, L., Cellone, S., & Torres, A. F. (2019). Indications for transit-timing variations in the exo-Neptune HAT-P-26b. *Astronomy and Astrophysics*, 628, Article A116. <https://doi.org/10.1051/0004-6361/201731966>
- Zechmeister, M., & Kürster, M. (2009). The generalised Lomb-scargle periodogram. A new formalism for the floating-mean and Keplerian periodograms. *Astronomy and Astrophysics*, 496(2), 577-584. <https://doi.org/10.1051/0004-6361:200811296>